# Kinetic Characterization of the ATPase Cycle of the DnaK Molecular Chaperone[†]

Rick Russell, Robert Jordan,[‡] and Roger McMacken*

*Department of Biochemistry, School of Hygiene and Public Health, Johns Hopkins University, Baltimore, Maryland 21205*

*Received August 14, 1997; Revised Manuscript Received November 7, 1997*

ABSTRACT: DnaK, the prototype Hsp70 protein of *Escherichia coli*, functions as a molecular chaperone in protein folding and protein disassembly reactions through cycles of polypeptide binding and release that are coupled to its intrinsic ATPase activity. To further our understanding of these processes, we sought to obtain a quantitative description of the basic ATPase cycle of DnaK. To this end, we have performed steady-state and pre-steady-state kinetics experiments and have determined rate constants corresponding to individual steps in the DnaK ATPase cycle at 25 °C. Hydrolysis of ATP proceeds very slowly with a rate constant ($k_{hyd} \approx 0.02$ min$^{-1}$) at least 10-fold smaller than the rate constant for any other first-order step in the forward reaction pathway. The ATP hydrolysis step has an activation energy of 26.2 ± 0.4 kcal/mol and is rate limiting in the steady-state under typical *in vitro* conditions. ATP binds with unusual strength to DnaK, with a measured $K_D \approx 1$ nM. ADP binds considerably less tightly than ATP and dissociates from DnaK with a $k_{off}$ of ∼0.4 min$^{-1}$ (compared with a $k_{off}$ of ∼0.008 min$^{-1}$ for ATP). However, in the presence of physiologically relevant concentrations of inorganic phosphate ($P_i$), the release of ADP from DnaK is greatly slowed, approximately to the rate of ATP hydrolysis. Under these conditions, the ADP-bound form of DnaK, the form that binds substrate polypeptides most tightly, was found to represent a significant fraction of the DnaK population. The slowing of ADP release by exogenous $P_i$ is due to thermodynamic coupling of the binding of the two ligands, which produces a coupling energy of ∼1.6 kcal/mol. This result implies that product release is not strictly ordered. In the absence of exogenous inorganic phosphate, $P_i$ product, by virtue of its higher $k_{off}$, is released prior to ADP. However, at physiological concentrations of inorganic phosphate, the alternate product release pathway, whereby ADP dissociates from a ternary DnaK·ADP·$P_i$ complex, becomes more prominent.

*Escherichia coli* DnaK protein is a well-characterized member of the highly conserved Hsp70 class of proteins. In addition to functioning in response to heat and certain other forms of stress, many Hsp70 family members, including DnaK, are expressed constitutively, and have been implicated in an array of protein metabolic processes (for recent reviews, see refs *1*−*3*). These include the folding of nascent polypeptides (*4*, *5*), intracellular protein trafficking (*6*, *7*), protein degradation (*8*), and disassembly of certain native protein complexes, including one formed at the bacteriophage λ replication origin (*9*, *10*). In all of these processes, the participating Hsp70 proteins are thought to act as molecular chaperones, undergoing multiple cycles of binding to and release from polypeptide substrates.

Hsp70 proteins are separable by limited proteolysis into two stable domains (*11*). The C-terminal domain has been shown to bind synthetic peptides in an extended conformation (*12*, *13*), a reaction which is thought to mimic the binding of physiological substrates. The N-terminal domain (*14*, *15*) is the site of the weak intrinsic ATPase activity associated with each Hsp70 protein. Through work on various Hsp70 family members, it has become clear that the two domains interact and that the peptide binding and release cycle is closely coupled to the ATP binding and hydrolysis cycle. ATP-binding induces the rapid release of bound peptide (*16*−*20*), but the ATP-bound state of Hsp70 binds peptide rapidly as well (*17*, *19*), and peptide, once bound, stimulates ATP hydrolysis (*21*, *22*). Furthermore, the degree of stimulation is dependent on the amino acid sequence of the peptide (*22*). In the ATP-bound form, Hsp70s may be considered to be as "sampling" peptides, until a favorable interaction causes hydrolysis of ATP, which results in a stable Hsp70−peptide complex. Since dissociation of peptide is dramatically slower from the ADP-bound form of Hsp70, it has been proposed that dissociation of Hsp70−peptide complexes *in vivo* results from the rebinding of ATP following ADP release (*18*).

An additional level of regulation is provided in *E. coli* by the cochaperones DnaJ and GrpE, which modulate the activity of DnaK by affecting specific steps of the ATPase cycle. Various *in vitro* assays for DnaK activity are dependent on DnaJ, and either dependent on or stimulated by GrpE. These include initiation of phage λ and phage P1 DNA replication (for review, see ref *23*), and the refolding of denatured luciferase (*24*). DnaJ has been shown to stimulate the ATPase activity of DnaK by accelerating the hydrolysis step or a first-order step preceding hydrolysis (*25*, *26*), while GrpE increases the rate of ADP release (*25*, *27*).

[†] This research was supported by NIH grant GM36526 from the National Institute of General Medical Sciences. We also acknowledge support of R.R. by NIEHS Training Grant ES07141 and of the oligonucleotide synthesis facility by NIEHS Center Grant ES-03819.

* To whom correspondence should be addressed. Tel: 410-955-3949. Fax: 410-955-2926. E-mail: rmcmacke@jhsph.edu.

[‡] Present address: Department of Microbiology, University of Pennsylvania School of Medicine, Philadelphia, Pennsylvania 19104.

S0006-2960(97)02025-4 CCC: $15.00 
Published on Web 01/13/1998

Like Hsp70, the DnaJ cochaperone has been found in a variety of organisms, and its capacity to interact functionally with specific Hsp70 proteins appears to have been conserved. For example, the DnaJ homolog Ydj1p has been shown to stimulate the steady-state ATPase activity of Ssa1p, a cytosolic Hsp70 from yeast (*28*). Additionally, it has recently been shown that the Hsp70-mediated uncoating of clathrin-coated vesicles requires auxilin, a 104-kDa protein that is partially homologous to DnaJ (*29*, *30*). To date, no GrpE homologue has been found in the cytosol of eukaryotic cells, but mitochondria have been found to contain a GrpE-related cochaperone that has functional properties similar to bacterial GrpE (*31*, *32*).

In this report, we describe a kinetic characterization of the ATPase cycle of DnaK. This information provides a quantitative framework for evaluating the effects of DnaJ, GrpE, and peptide substrates on this cycle. We find that DnaK binds ATP very tightly, with an estimated $K_D$ of 1 nM. We demonstrate further that ATP hydrolysis by DnaK is slow and that the hydrolysis step is essentially rate limiting in steady state at low concentrations of inorganic phosphate ($P_i$).[1] We find, however, that the release of ADP product is greatly slowed by the presence of exogenous $P_i$, such that ADP dissociation becomes partially rate limiting at physiological $P_i$ concentrations (5−10 mM). In further support of this conclusion, we also demonstrate that the nucleotide state of DnaK under steady-state conditions is increasingly ADP bound as the concentration of $P_i$ is raised. This provides additional evidence for the existence of a balance in the intrinisic rates of ATP hydrolysis and product release. The ramifications of this finding on the polypeptide-binding state of DnaK *in vivo* are discussed.

## MATERIALS AND METHODS

*Materials*. Materials and their sources were AMP-PNP (Boehringer Mannheim); polyethyleneimine-cellulose thin layer chromatography sheets (EM Industries); ATP (Pharmacia Biotech); ADP (Calbiochem); Synchropak AX-100 HPLC column (Synchrom, Inc.); 12−14 kDa MWCO dialysis membrane (Spectra-Por); [α-$^{32}$P]ATP (denoted ATP*) (>3000 Ci/mmol) and [γ-$^{32}$P]ATP (>3000 Ci/mmol) (Amersham); and nitrocellulose filters (type HA, 0.45 μm pore size, Millipore). All other biochemicals were from Sigma.

*Overexpression and Purification of DnaK Protein*. DnaK was purified to homogeneity (>98% pure) from *E. coli* strains carrying plasmids designed for overexpression of a cloned *dnaK* gene. Particular care was taken during purification to reduce the level of contaminating peptides that are often found in DnaK preparations. A detailed description of pRLM163 plasmid construction and our protocols for DnaK expression and purification are available as Supporting Information.

*Removal of Bound Nucleotide*. Nucleotide removal from DnaK preparations was accomplished using the protocol of Gao et al. (*33*) by competing off bound nucleotide with excess AMP-PNP, followed by dialysis to remove less tightly bound AMP-PNP. Three days of dialysis with daily buffer changes was sufficient to reduce the nucleotide content to <0.09 mol/mol of DnaK, with the remaining nucleotide present as AMP-PNP.

Alternatively, ADP was removed by dialyzing DnaK at 4 °C against 1000 vol of buffer containing 20 mM imidazole/HCl, pH 7.3, 2 mM EDTA, and 10% (v/v) glycerol. With one buffer change per day, 4 days was sufficient to remove >95% of bound ADP (to <0.01 mol/mol of DnaK).

*Preparation of [α-$^{32}$P]ADP*. [α-$^{32}$P]ADP (denoted ADP*) was prepared by incubating 30 μCi of ATP* in 20 μL of HM buffer (40 mM Hepes/KOH, pH 7.6, 11 mM magnesium acetate, and 200 mM potassium glutamate) with 1 pmol of DnaK for 5 hours at 37 °C. Residual ATP was removed by anion-exchange chromatography on DEAE-Sephadex A-25 with a linear gradient from 0.1 to 0.8 M triethylammonium bicarbonate. Fractions containing the peak of ADP were evaporated to dryness in a Speedvac. On the basis of TLC analysis, the ADP preparation was estimated to be >95% pure.

*Measurement of Steady-State ATPase Activity*. Reaction mixtures (75 μL) contained HM buffer, 50 μg/mL of BSA, 1 nM DnaK, 3 μCi/mL of ATP* (1 nM), and 2−80 nM unlabeled ATP. DnaK was preincubated at the indicated reaction temperature (typically 25 °C) for 5 min, and hydrolysis reactions were initiated with the addition of ATP. Samples from the reaction mixture (≥6 per reaction) were quenched at various times by adding 8 μL of the reaction mixture to 2 μL of 1 N HCl, and were placed on ice. Each sample (2 μL) was spotted on polyethylenimine-cellulose TLC sheets, which were developed in 1 M formic acid, 0.5 M LiCl. The fraction of nucleotide present as ADP was determined using a Fuji BAS 1000 imager. Hydrolysis of ATP was not allowed to exceed 12%. Data were corrected for the background level of ADP (typically 1−4%) present in commercially available ATP* and for a fraction (∼5%) of unidentified radioactive material that remains at the origin in the TLC analysis and does not interact stably with DnaK (data not shown). At each concentration of ATP, $v_o$ was determined from a linear regression analysis. $K_M$ and $k_{cat}$ were determined by fitting a plot of ($v_o$/[DnaK]) against the concentration of ATP to the Michaelis−Menten equation using the nonlinear regression program Enzfitter (Biosoft, Cambridge, U.K.).

*Measurement of Single-Turnover ATPase Activity*. Reaction mixtures (120 μL) and reactions were essentially identical to those described for measurement of steady-state ATPase activity, except that DnaK was present in substantial excess over ATP (typically 1−5 μM DnaK and 5−30 nM ATP*), and ATP hydrolysis was followed to completion. The conversion to ADP was plotted as a function of time and fit to a first-order rate equation using Enzfitter. At least two concentrations of DnaK over a ≥2-fold range were used to ensure that saturation with DnaK had been achieved.

*Measurement of ATP Synthesis*. Reactions were performed in HM buffer (45 μL) containing DnaK (2 μM) and ADP* (130 nM; 0.01 μCi). Where indicated, reaction mixtures also contained either DnaJ (2 μM) or GrpE (5 μM). The reaction mixture was preincubated for 5 min at 25 °C, and the ATP synthesis reaction was initiated by the addition of potassium phosphate to a final concentration of 50 mM.

[1] Abbreviations: $P_i$, inorganic phosphate; AMP-PNP, 5′-adenylyl imidodiphosphate; ATP*, [α-$^{32}$P]ATP; ADP*, [α-$^{32}$P]ADP; Hepes, 4-(2-hydroxyethyl)piperazine-1-ethanesulfonic acid; DTT, dithiothreitol; EDTA, ethylenediaminetetraacetic acid; Tris, tris(hydroxymethyl)-aminomethane; BSA, bovine serum albumin; DEAE-, diethylaminoethyl-; TLC, thin-layer chromatography.

The fraction of nucleotide present as ATP and ADP was determined at various times as described for measurement of steady-state ATPase activity.

*Measurement of ATP Release*. Reactions were performed in HM buffer (120 $\mu$L final volume), with DnaK (2 $\mu$M) present in excess over ATP* (5−30 nM). After a 5 min preincubation of DnaK at 25 °C, ATP* was added and further incubated for 2 min to allow for binding of ATP to DnaK. The release of bound ATP was then rendered irreversible by the subsequent addition of a large excess of unlabeled ATP (5 mM). Control experiments indicated that ATP* was not reactive when added simultaneously with chase ATP. Data were obtained and analyzed as described for single-turnover ATPase measurements.

*Measurement of ADP Release.* Reactions (180 $\mu$L) were performed in HM buffer, with DnaK (2 $\mu$M) present in excess over ADP* (25 nM). After a 5 min preincubation of DnaK in HM buffer at 25 °C, ADP* was added, and the reaction mixtures were incubated for an additional 2 min to allow for ADP* binding, at which time unlabeled ADP was added to a final concentration of 5 mM. Where noted, potassium phosphate was added 30 s prior to unlabeled ADP. At various times after the addition of unlabeled ADP, portions (15 $\mu$L) of the reaction mixture were spotted on a nitrocellulose filter under gentle vacuum and washed with 1 mL of HM buffer. Filters were dried and counted in a scintillation counter. The fraction of bound ADP* was corrected for background (∼2%), plotted as a function of time, and fit to a single exponential decay using Enzfitter.

*Isolation of DnaK·Nucleotide Complexes*. To determine the identity of the nucleotide bound to DnaK in steady-state ATPase experiments, 50 $\mu$L portions of a 300 $\mu$L reaction mixture that initially contained 100 $\mu$M ATP* (69 $\mu$Ci) were removed at various times (30, 90, 150, and 210 min after the start of the reaction) and applied to a 24 mL Superose 12 column at 4 °C. The columns were eluted at a flow rate of 0.5 mL/min in HM buffer, and fractions (0.2 mL) that contained DnaK protein, as monitored by absorbance at 280 nm, were immediately quenched with 50 $\mu$L of 1 N HCl and analyzed by TLC. The peak of DnaK·ATP consistently eluted approximately 0.2 mL ahead of the peak of DnaK·ADP (elution volumes were 11.4 and 11.6 mL, respectively). Therefore, to obtain an accurate determination of the ATP/ADP ratio of the bound nucleotide, it was inappropriate to analyze a single individual fraction. Rather, the amounts of ATP and ADP in several fractions encompassing the peak of each nucleotide were summed to obtain values for the total amounts of each nucleotide recovered bound to DnaK; the amount of ATP was then divided by that of ADP to obtain a ratio.

Control experiments indicated that when exogenous $P_i$ was absent from both the reaction buffer and the column running buffer, a significant portion of the DnaK·ADP complex dissociated during the column run. This problem was circumvented by including 5 mM phosphate in the column running buffer, which reduced complex dissociation to insignificant levels.

*Measurement of the Rate Constant for ATP Binding*. Reactions (180 $\mu$L) were performed in HM buffer containing 50 $\mu$g/mL BSA, 0.02−1 $\mu$M DnaK and limiting ATP* (3 nM). After preincubating DnaK for 5 min, reactions were initiated with the addition of ATP*. Portions removed at various times thereafter were quenched by one of two methods. At low concentrations of DnaK, the binding reaction was sufficiently slow to enable collection of data by filter binding, as described above. At higher concentrations of DnaK, portions of the reaction mixture were quenched with the addition of unlabeled ATP to a final concentration of 5 mM, competitively blocking additional ATP* from binding DnaK. Bound ATP* was quantitatively converted to ADP* with a 15 min incubation at 25 °C in the presence of 2 $\mu$M DnaJ. Each sample was analyzed by TLC for the amounts of ATP* and ADP* present. For both quench methods, data were fit to a first-order rate equation using Enzfitter to determine $k_{obs}$, the pseudo-first-order rate constant. The binding reactions were performed over an intermediate range of DnaK concentrations with no significant differences in the results obtained. Experiments measuring the affinity of $P_i$ for DnaK were performed similarly, with unlabeled ATP as a quench.

Scheme 1

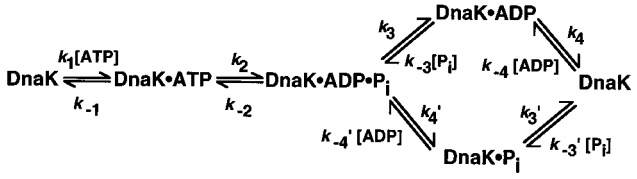


*Measurement of the Rate Constant for ADP Binding in the Presence of Inorganic Phosphate.* Reactions (180 $\mu$L) were performed in HM buffer containing 50 $\mu$g/mL BSA, 0.02−0.15 $\mu$M DnaK, and limiting ADP* (3 nM). DnaK was preincubated 5 min with 5 mM potassium phosphate, and the binding reaction was subsequently initiated with the addition of ADP*. Samples taken at various times thereafter were quenched by filter binding and processed as described for measurement of the rate of ATP binding.

*Analysis of Error*. Results are reported plus or minus 1 standard deviation resulting from the fit of the data, with propagation of error through any subsequent calculations. Rate constants measurable with a single time course (i.e., $k_2$, $k_4$, $k_{-1}$) are reported as the average of 3−5 independent determinations. Rate and equilibrium constants requiring a fit to $k_{obs}$ (i.e., $k_1$, $k'_{-4}$, $K_3$) are reported plus or minus 1 standard deviation from the secondary fit, using all available values of $k_{obs}$.

## RESULTS

Steady-state and pre-steady-state kinetic techniques were used to measure rate constants corresponding to individual steps in the ATPase cycle of DnaK, and results are interpreted in the context of Scheme 1.

*Preparation of DnaK*. To obtain the large quantities of protein required for experiments with protein in excess of ATP, the *dnaK* gene was inserted into a thermoinducible expression vector (pRLM 163). For some experiments, protein was expressed from pMOB45*dnaK*$^+$ (see Materials and Methods). Some preparations of DnaK, purified using a modification of the standard protocol reported here, were found to have anomalous ATPase activities. These included a "burst" in single-turnover assays, and a higher than normal steady-state activity. In at least one case, this is suspected to be the result of a small amount of a contaminating ATPase, since application of the preparation to a column containing

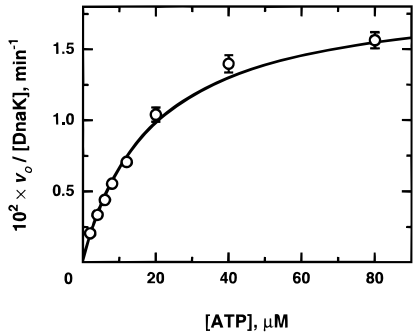


FIGURE 1: Steady-state ATPase activity of DnaK. Reaction mixtures (75 $\mu$L) contained 1 nM DnaK and 2−80 nM ATP, including 0.3 $\mu$Ci of ATP*. Initial rates were determined from a least-squares linear-regression analysis of the data, and are plotted as rate divided by DnaK concentration, with error bars of ±1 standard deviation. The curve represents a least-squares fit to the Michaelis−Menton equation and yielded $K_M$ = 19 nM and $k_{cat}$ = 0.019 min$^{-1}$.

immobilized polyclonal antibody to DnaK resulted in resolution of a substantial portion of the anomalous ATPase activity from DnaK protein (data not shown). All assays measuring ATP hydrolysis were performed with DnaK preparations that were essentially free of contaminating ATPase activity. Additionally, all pre-steady-state experiments in which the observed rate constants were expected to be dependent on protein concentration were performed with DnaK preparations from which nucleotide had been removed essentially as described (*33*).

*Measurement of Steady-State ATPase Activity*. To establish an overall picture of the ATPase reaction to which measurements of individual rate constants might be compared, a steady-state analysis was performed at 25 °C (Figure 1). The values obtained for $K_M$ (19 ± 2 nM) and $k_{cat}$ (0.019 ± 0.001 min$^{-1}$) are in reasonable agreement with previous determinations (*34*). The standard assay buffer contained 200 mM potassium glutamate, but replacement with an equivalent concentration of potassium chloride had little or no effect on the steady-state parameters (data not shown). Additionally, both $K_M$ and $k_{cat}$ were found to be independent of the concentration of potassium ion between 20 and 200 mM (data not shown).

*Determination of $k_2$, the Rate Constant for Hydrolysis of ATP*. With limiting ATP*, the reaction can be represented as two sequential steps (eq 1).

$$\text{DnaK} + \text{ATP} \underset{k_{-1}}{\overset{k_1}{\rightleftharpoons}} \text{DnaK·ATP} \underset{k_{-2}}{\overset{k_2}{\rightleftharpoons}} \text{DnaK·ADP·P}_i \quad (1)$$

However, at high concentrations of DnaK, binding will be rapid, in effect reducing the process to one rate-determining step. Under these conditions, the ADP concentration is expected to vary with time according to eq 2, where [ADP$_t$] is the concentration at a given time; [ADP$_\infty$] is the final concentration of ADP; $C$ is a constant that corresponds to a small amount of residual contaminating ATPase activity (accounting for 1−2% of the total ATP* hydrolyzed) that is too fast to be measured accurately and is therefore not included in the time course; and $k_{obs}$ is the observed first order rate constant, which is hyperbolic with respect to [DnaK] to a value corresponding to the sum of $k_2$ and $k_{-2}$.

$$[\text{ADP}_t] = [\text{ADP}_\infty](1 - e^{-k_{obs}t}) + C \quad (2)$$

Table 1: Summary of Rate and Equilibrium Constants

| | |
|---|---|
| $k_1$ (M$^{-1}$ min$^{-1}$) | (8.0 ± 0.3) × 10$^6$ |
| $k_{-1}$ (min$^{-1}$) | 0.008 ± 0.002 |
| $K_1$ (nM)[a] | 1.0 ± 0.3 |
| $k_2$ (min$^{-1}$) | 0.018 ± 0.004 |
| $k_{-2}$ (min$^{-1}$) | ≤0.0004 |
| $K_3$ ($k_3/k_{-3}$) (mM) | 0.22 ± 0.02 |
| $K'_3$ ($k'_3k'_{-3}$) (mM) | 2.5 ± 0.3 |
| $k_4$ (min$^{-1}$) | 0.37 ± 0.05 |
| $k'_4$ (min$^{-1}$) | 0.019 ± 0.003 |
| $k'_{-4}$ (M$^{-1}$ min$^{-1}$) | (1.6 ± 0.3) × 10$^7$ |
| $K_4$ (nM)[b] | 25 ± 7 |
| $K'_4$ (nM)[a] | 1.2 ± 0.3 |
| $k_{cat}$ (min$^{-1}$) | 0.019 ± 0.001 |
| $K_M$ (nM) | 19 ± 2 |

[a] $K_1$ and $K'_4$, the equilibrium dissociation constants for ATP and ADP in the presence of saturating $P_i$, respectively, were calculated by dividing each rate constant for release by the respective rate constant for binding. [b] $K_4$, the equilibrium dissociation constant for ADP in the absence of $P_i$, was calculated from the determined dissociation rate constant ($k_4$) and the rate constant for binding in the presence of $P_i$ ($k'_{-4}$). It was assumed that $P_i$ has little or no effect on the rate of ADP binding, in agreement with the lack of dependence of the observed binding rate on [$P_i$] (see text).

No net conversion of ADP to ATP was detected in the presence of ADP* and saturating concentrations of $P_i$ (data not shown). The presence of the DnaJ or GrpE cochaperones in the reaction mixture did not elicit detectable ATP synthesis by DnaK. Using a conservative value for our ATP detection limit, we estimate that $k_{-2} \leq 4 \times 10^{-4}$ min$^{-1}$ (Table 1). Our inability to detect synthesis of ATP by DnaK is not surprising. A similar finding has previously been made for bovine Hsc70 protein (*35*). Our results indicate that $k_{-2}$ is insignificant relative to $k_2$, so $k_{obs} = k_2$ when DnaK is saturating. At a DnaK concentration of 2 $\mu$M, $k_{obs}$ was determined to be 0.018 ± 0.004 min$^{-1}$ (Figure 2A). Varying the concentration of DnaK from 0.2 to 5 $\mu$M had no significant effect on $k_{obs}$ (data not shown), suggesting that $k_2 \approx 0.018$ min$^{-1}$. This is essentially equal to $k_{cat}$ (0.019 min$^{-1}$) measured in steady state, indicating that hydrolysis of ATP, or a first-order step that precedes hydrolysis, is rate limiting for the DnaK ATPase cycle under the conditions of Figures 1 and 2.

It was reported that the steady-state ATPase activity of DnaK displays a steep temperature dependence, with an 80-fold increase in rate from 20 to 53 °C (*36*). We examined the effect of temperature on the hydrolysis step specifically by performing single-turnover ATPase reactions at a saturating DnaK concentration as a function of temperature in the range 15−55 °C. At temperatures from 15 to 40 °C, reactions followed first-order kinetics, and the Arrhenius plot is linear (Figure 2B). The activation energy, $E_a$, was determined to be 26.2 ± 0.4 kcal/mol.

At temperatures greater than 40 °C, the reaction was biphasic, with a lag that was dependent on DnaK concentration. Calorimetry experiments have shown that the N-terminal domain of DnaK undergoes an apparent unfolding transition at ∼43 °C in the absence of nucleotide (*37*). This phenomenon may decrease the active DnaK concentration, making the rate of binding of ATP kinetically significant and producing a lag. The second of the two observed rate constants obtained at 45 and 55 °C are included in Figure 2B, but data obtained at these temperatures were excluded when determining $E_a$.

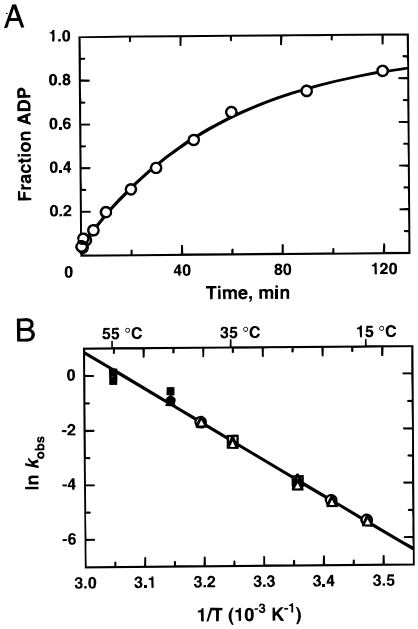


FIGURE 2: Single-turnover ATPase activity of DnaK. (A) Reaction mixtures (120 $\mu$L) contained 2 $\mu$M DnaK and 3 nM ATP, including 1.08 $\mu$Ci of ATP*. The curve represents a least-squares fit to a first-order rate equation and produces $k_{obs} = 0.018$ min$^{-1}$. (B) Single-turnover ATPase assays were performed as a function of temperature, with reactions containing 3 nM ATP* and 1 $\mu$M DnaK (○), 2 $\mu$M DnaK (△), or 5 $\mu$M DnaK (□). Observed first-order rate constants were determined as for panel A and are shown as an Arrhenius plot. $E_a$, the activation energy for the reaction, was determined from a least-squares linear regression of the data to be 26.2 ± 0.4 kcal/mol. Reactions in which a kinetic lag was observed (closed symbols; see Results) were not used in the determination of $E_a$.

*Determination of the Rate Constant for ATP Binding.* If binding of ATP to DnaK proceeds in a single step, the relevant scheme is represented by eq 3 when DnaK is present in excess.

$$\text{ATP} \underset{k_{-1}}{\overset{k_1[\text{DnaK}]}{\rightleftharpoons}} \text{DnaK·ATP} \xrightarrow{k_2} \text{DnaK·ADP·P}_i \qquad (3)$$

Under conditions in which binding of ATP is fast relative to hydrolysis and to ATP release, the formation of a DnaK·ATP complex will be approximated by a single exponential function, where $k_{obs}$ is composed of rate constants representing both steps (eq 4).[2]

$$k_{obs} \approx k_1[\text{DnaK}] + k_{-1} + k_2 \qquad (4)$$

To measure the kinetics of ATP binding, DnaK was titrated in the presence of limiting ATP*, and at various times after mixing the two components, the relative concentration of the DnaK·ATP* complex was determined by filter binding (Figure 3A). At DnaK concentrations >0.4 $\mu$M, the reaction was too fast to measure accurately by filter binding. However, reactions containing 0.4−1 $\mu$M DnaK were performed by quenching time-point samples with excess unlabeled ATP, to prevent further binding of ATP*. Bound ATP* was quantitatively converted to ADP* in a subsequent incubation with DnaJ, and the fraction of ATP* converted to ADP* was taken as a measure of the fraction of input ATP* that was bound by DnaK at a given time.

[2] Equation 4 includes both $k_{-1}$ and $k_2$ because they are of comparable magnitude (see below) and, therefore, both contribute to $k_{obs}$ at low [DnaK].

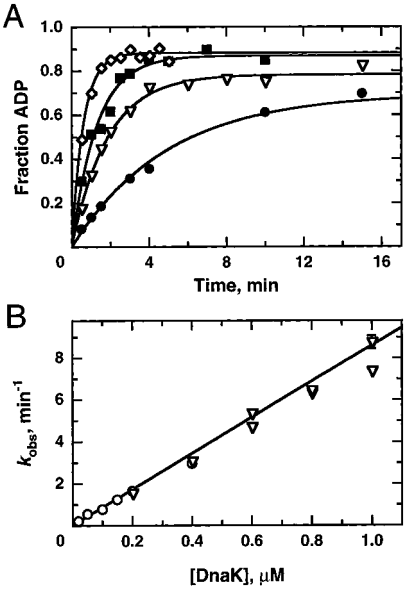


FIGURE 3: Association kinetics of DnaK and ATP. (A) Reaction mixtures (180 $\mu$L) contained 3 nM ATP* (1.6 $\mu$Ci) and 0.02 $\mu$M DnaK (●), 0.05 $\mu$M DnaK (▽), 0.10 $\mu$M DnaK (■), or 0.15 $\mu$M DnaK (◆). Samples were quenched by filter binding. The curves shown depict least-squares fits to a first-order rate equation. (B) Pseudo-first-order rate constants are plotted against [DnaK]. Binding reactions were quenched either by filter binding (○) or by the addition of unlabeled ATP (▽), as described in Materials and Methods. The second-order rate constant for association of ATP and DnaK was determined from the slope of a least-squares linear-regression analysis of the data to be 8.0 × $10^6$ $M^{-1}$ $min^{-1}$. The $y$-intercept ($k_{-1} + k_2$) was ≤0.15 $min^{-1}$.

To obtain a value for the second-order rate constant for binding, $k_1$, $k_{obs}$ was plotted as a function of [DnaK] (eq 4). This yielded a reasonable fit to a line with a slope equal to $k_1$ and a $y$-intercept of $k_{-1} + k_2$ (Figure 3B). On the basis of this fit, $k_1$ was determined to be (8.0 ± 0.3) × $10^6$ $M^{-1}$ $min^{-1}$, and $k_{-1} + k_2$ was ≤0.15 $min^{-1}$. Fitting a line only to data from assays performed with one quench method (filter binding) or with the other (excess unlabeled ATP) yielded similar results. Furthermore, over the limited range of DnaK concentrations in which both methods were performed, the results agreed well.

*Direct Measurement of ATP Release.* While the previous experiment provided a reasonable estimate for $k_1$, it provided only an upper limit for $k_{-1}$. To obtain a value for the rate constant for ATP release, a pulse-chase experiment was performed. Limiting ATP* was allowed to bind to DnaK for 1 min, after which excess unlabeled "chase"ATP was added. Following the fraction of ATP* that is converted to ADP* with time (Figure 4) provides two methods for determining $k_{-1}$. The DnaK·ATP* complex may decompose in two ways, either through hydrolysis or release of ATP* (eq 5).

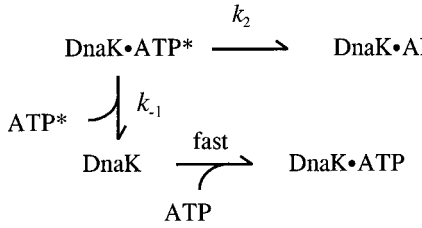


(5)

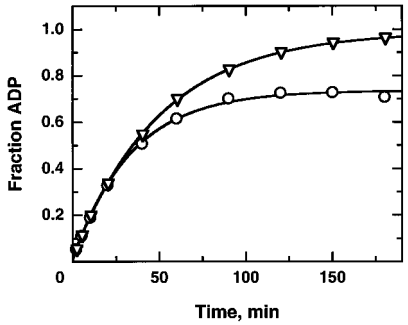


FIGURE 4: Measurement of the rate constant for dissociation of ATP from DnaK. Reaction mixtures (120 $\mu$L) contained 2 $\mu$M DnaK and 3 nM ATP* (1.08 $\mu$Ci). Conversion of ATP to ADP was followed in the presence (○) or absence (▽) of 5 mM unlabeled ATP, added after a 1 min incubation of DnaK and ATP*. The curves represent least-squares fits to a first-order rate equation, yielding $k_{obs} = 0.030$ min$^{-1}$ (in the presence of unlabeled ATP) and 0.020 min$^{-1}$ (in the absence of unlabeled ATP). Final values for the conversion to ADP were 0.73 ± 0.02 (○) and 0.990 ± 0.004 (▽).

In the presence of unlabeled chase ATP, hydrolysis will proceed, not to completion, but to a final value that reflects the partitioning of the hydrolysis and release reactions (eq 6).

$$\frac{[\text{ADP*}]}{[\text{ADP*}] + [\text{ATP*}]} = \frac{k_2}{k_2 + k_{-1}} \qquad (6)$$

By determining the plateau level of hydrolysis and using the independently obtained value of $k_2$, $k_{-1}$ can be determined. This analysis yielded a value for $k_{-1}$ of 0.0076 ± 0.0016 min$^{-1}$. If DnaK is not present at saturating concentrations, not all the ATP* will be bound initially, causing an overestimation of $k_{-1}$. To test this possibility, the DnaK concentration was raised 2.5-fold to 5 $\mu$M, and $k_{-1}$ was determined as before, but no significant change in the ATP release rate was found (data not shown).

Additionally, $k_{-1}$ may be determined from $k_{obs}$ in the presence of unlabeled chase ATP, since the observed rate constant will be equal to the sum of the rate constants for the two pathways, i.e., $k_{obs} = k_2 + k_{-1}$. Analysis using this method yielded a value for $k_{-1}$ of 0.010 ± 0.0014 min$^{-1}$, in reasonable agreement with the value obtained using eq 6. From the results of Figures 3 and 4, the $K_D$ for ATP dissociation from DnaK can be calculated using the relationship $K_D = k_{-1}/k_1$, which provides a $K_D$ of 1.0 ± 0.3 nM.

*Analysis of $P_i$ and ADP Release*. It has been shown for Hsc70 that product release may be approximated as ordered, with $P_i$ released first, followed by ADP (*35*). Furthermore, it was determined that $P_i$ release is partially rate limiting in the steady state, with a rate constant approximately equal to that of ATP hydrolysis. We attempted to determine the rate constant for $P_i$ release ($k_3$) by incubating limiting [$\gamma$-$^{32}$P]-ATP with DnaK, and monitoring release of $P_i$ following hydrolysis of ATP by binding DnaK to nitrocellulose filters. However, the time course of the decay of bound $P_i$ was adequately described by a single exponential with $k_{obs}$ essentially equal to $k_2$, the rate constant for hydrolysis (data not shown). This suggests that $P_i$ release is fast relative to hydrolysis, consistent with the idea that ATP hydrolysis is fully rate limiting for DnaK under these conditions (i.e., $k_2 = k_{cat}$). Additional experiments in the presence of DnaJ, which increases $k_2$ but not $k_3$ (data not shown), suggested that the rate constant for $P_i$ release is >0.7 min$^{-1}$.

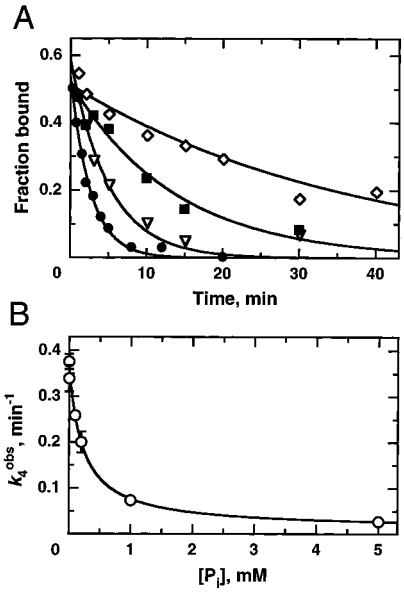


FIGURE 5: $P_i$ inhibits the release of ADP from DnaK. (A) Reaction mixtures (180 $\mu$L) contained 2 $\mu$M DnaK and 25 nM ADP* (0.11 $\mu$Ci), but with either no potassium phosphate (●), or with 0.2 mM (▽), 1 mM (■), or 5 mM potassium phosphate (◇). Fractions of ADP* bound were determined by filter binding, performed as described in Materials and Methods. The curves represent least-squares fits to a single exponential decay. (B) The observed rate constants are plotted as a function of [$P_i$]. The curve depicts a least-squares fit to a rate equation (eq 8), as described in Results.

To determine whether $P_i$ affects ADP release from DnaK, filter binding assays were performed in the presence of various concentrations of potassium phosphate. Limiting ADP* was incubated with DnaK, followed by the addition of excess unlabeled ADP. The time courses of ADP release were fitted to single exponential functions, and $k_4^{obs}$ was found to decrease with increasing concentrations of $P_i$ (Figure 5A). However, even in the presence of saturating concentrations of potassium phosphate (e.g., 20 mM), $k_4^{obs}$ was not zero. This indicates that product release from DnaK is not strictly ordered. Data were therefore interpreted in the context of a model in which ADP is released from DnaK in the presence or absence of $P_i$, but with a much smaller rate constant in its presence (i.e., $k_4' \ll k_4$). In eq 7, $K_3 = k_3/k_{-3}$ and $P_i$ binding and release are assumed to be in rapid equilibrium relative to ADP release, consistent with the observation that the time courses were adequately fit by single exponential functions.

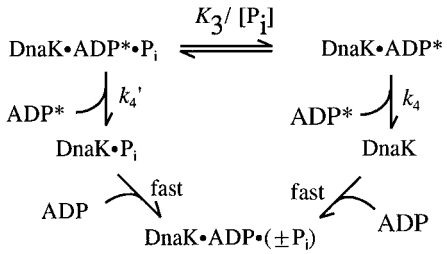


(7)

To determine values for $k_4$, $k_4'$, and $K_3$, $k_4^{obs}$ was plotted as a function of [$P_i$] and fit to an equation describing parallel release pathways with an internal rapid equilibrium (eq 8, results are shown in Figure 5B).

$$k_4^{obs} = \frac{k_4'[P_i] + k_4 K_3}{K_3 + [P_i]} \qquad (8)$$

Table 2: Determination of the Form of Nucleotide Bound to DnaK in the Steady State

| $[P_i]$ mM | $k_{cat,obs}$ ($min^{-1}$)[a] | ATP/ADP[b] | $k_2$ ($min^{-1}$)[c] | $k_4^{obs}$ ($min^{-1}$)[c] | $k_{cat,calc}$ ($min^{-1}$)[d] |
|---|---|---|---|---|---|
| 0 | 0.017 | 13 | 0.018 | 0.24 | 0.017 |
| 0.5 | 0.014 | 5.1 | 0.017 | 0.088 | 0.016 |
| 2 | 0.012 | 1.4 | 0.020 | 0.028 | 0.013 |
| 5 | 0.0094 | 1.6 | 0.015 | 0.025 | 0.011 |

[a] $k_{cat,obs}$ was determined under steady-state conditions (2 $\mu$M DnaK, 100 $\mu$M ATP) (data not shown). [b] The ATP/ADP ratio of DnaK-associated nucleotide in steady state was determined following isolation of protein−nucleotide complexes by gel chromatography as described in Materials and Methods. [c] $k_2$ and $k_4^{obs}$, the rate constants for ATP hydrolysis and ADP release, respectively, were calculated from $k_{cat,obs}$ and the ratio of bound ATP to ADP as described in Results. [d] Expected values of $k_{cat}$ were calculated using the determined values of $k_2$ (0.018 $min^{-1}$) and of $k_4^{obs}$ (obtained from filter binding experiments; values for $k_4^{obs}$ with 0.5 mM and 2 mM $P_i$ were obtained by interpolation of the fit shown in Figure 5B). $P_i$ was assumed to have no effect on $k_2$. It was also assumed that only ATP hydrolysis and ADP release contribute significantly to the steady-state rate (see text), so $k_{cat,calc} = k_2 k_4^{obs}/(k_2 + k_4^{obs})$.

The fit yielded the following parameters: $k_4 = 0.37 \pm 0.03$ $min^{-1}$; $k_4' = 0.019 \pm 0.003$ $min^{-1}$; and $K_3 = 0.22 \pm 0.02$ mM. Thus, ADP is released ~20-fold slower in the presence of $P_i$ than in its absence. Since physiological levels of $P_i$ are greater than 20 times $K_3$, intracellular DnaK would be expected to contain bound $P_i$, in addition to bound ADP (in the absence of influence by cochaperones or polypeptide substrates). Under these conditions, ADP product will generally be released directly from a DnaK·ADP·$P_i$ ternary complex (i.e., via the lower pathway in Scheme 1). We conclude that the relative flux through the two possible product release pathways will be dependent on the concentration of $P_i$.

*Effect of $P_i$ on Steady-state ATPase Activity*. The previous experiment suggested that, at significant concentrations of $P_i$ (e.g., ~5 mM, 20-fold over $K_3$), the apparent rate of ADP release ($k_4^{obs}$) is approximately equal to $k_2$, the rate constant for hydrolysis. This predicts that, in the presence of high $[P_i]$ (high with respect to $K_3$), ADP release will be partially rate limiting under steady-state conditions. This prediction was tested directly in an experiment in which excess ATP* was incubated with DnaK, and at various times the identity of bound nucleotide was determined by chromatographic separation of protein from free nucleotide (*38*). In the absence of added $P_i$, nearly all the nucleotide bound to DnaK was ATP (Table 2). However, with increasing concentrations of $P_i$ in the reaction mixture, a significant fraction of the recovered nucleotide was ADP, demonstrating that hydrolysis is no longer fully rate limiting under these conditions.

The ratio of bound ATP to ADP, in combination with determination of $k_{cat}$ from the same reaction, permits calculation of $k_2$ and $k_4^{obs}$ at a given concentration of $P_i$. Assuming that only these two steps contribute to the overall rate of the reaction, $k_{cat}$ is a function of $k_2$ and $k_4^{obs}$ (eq 9).

$$k_{cat} = \frac{k_2 k_4^{obs}}{k_2 + k_4^{obs}} \quad (9)$$

Since the concentration of ATP in this steady-state experiment, 100 $\mu$M, greatly exceeded the measured $K_M$ of ~20 nM, then the measured rate divided by DnaK concentration is essentially equal to $k_{cat}$.[3] Additionally, if the steady-state assumption is applied, it can be shown that the ratio of $k_4^{obs}$ to $k_2$ is equal to the ratio of bound ATP to ADP (eq 10).

$$\frac{[DnaK\cdot ATP]}{[DnaK\cdot ADP]} = \frac{k_4^{obs}}{k_2} \quad (10)$$

Thus, once values for $k_{cat}$ and for the ATP:ADP ratio on DnaK are experimentally determined, there are two equations and two unknowns, permitting calculation of $k_2$ and $k_4^{obs}$.

We measured $k_{cat}$ for the steady-state ATPase activity of DnaK at a variety of $P_i$ concentrations and the results are summarized in Table 2. The addition of $P_i$ was observed to decrease $k_{cat}$ less than 2-fold. This decrease in rate was due primarily to a decrease in $k_4^{obs}$ (ADP release) rather than to an effect on the hydrolysis step specifically. Control experiments performed under single-turnover conditions confirmed that 10 mM $P_i$ has only a minimal effect on $k_2$, decreasing the observed rate of hydrolysis approximately 10−20%. Calculated values of $k_4^{obs}$ (Table 2) are in reasonable agreement with direct measurements from filter-binding experiments (Figure 5B). This steady-state determination may underestimate $k_4^{obs}$ at low concentrations of $P_i$, since a small amount of ATP hydrolysis during the 20 min procedure for isolation of DnaK may lead to a substantial decrease in the ATP/ADP ratio of bound nucleotide when the total amount of ADP is very low. This effect will be most significant for the reaction performed in the absence of exogenous $P_i$ and may explain the discrepancy in $k_4$ values between this experiment and the direct measurement from filter-binding experiments (Figure 5).

As an additional check of internal consistency, expected values of $k_{cat}$ were calculated as a function of $[P_i]$ using determined values of $k_2$ and $k_4^{obs}$ (in some cases $k_4^{obs}$ was interpolated from the curve fit to filter-binding data). This calculation was made assuming that only $k_2$ and $k_4^{obs}$ contribute to the steady-state rate and that, at $[P_i] \leq 5$ mM, $k_2$ is unaffected by $P_i$. The agreement between calculated and observed values of $k_{cat}$ was reasonably good (Table 2).

*Measurement of the Rate of ADP Binding*. Measurements of the ADP-binding rate were performed similarly to those for ATP, with the addition of limiting ADP* to DnaK, followed at various times by quenching of a portion of the reaction mixture by filter binding. In the absence of added $P_i$, we were unable to obtain an accurate estimate for $k_{-4}$, the ADP-binding rate constant, because, even at low concentrations of DnaK, the binding reaction equilibrated too quickly to measure by hand. However, in the presence of 5 mM $P_i$, which was essentially saturating for its inhibitory effect on ADP release (see Figure 5B), the process followed pseudo first-order kinetics, and a plot of $k_{obs}$ as a function

[3] $P_i$ competes with ATP for binding to DnaK (with $K_I \approx 2.5$ mM; see below) and would be predicted to affect the apparent $K_M$ for the hydrolysis reaction. At sufficiently high $[P_i]$, 100 $\mu$M ATP would not be saturating, invalidating the assumption of $k_{cat}$ conditions. The highest concentration of $P_i$ used (5 mM), however, is only about 2-fold greater than $K_I$. Under these conditions, the apparent $K_M$ would be predicted to increase about 3-fold to ~60 nM, still ~1000-fold less than the concentration of ATP used in this experiment. Thus, ATP remains saturating and $v_0/[DnaK] \approx k_{cat}$.

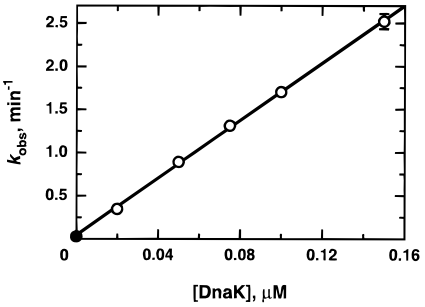


FIGURE 6: Measurement of the rate constant for association of ADP and DnaK. Reaction mixtures (180 $\mu$L) contained 3 nM ADP* (0.54 $\mu$Ci), 5 mM potassium phosphate, and 0.02−0.15 $\mu$M DnaK (○). Binding of ADP to DnaK was analyzed by filter binding as described in Materials and Methods. Observed rate constants were determined from least-squares fits to a first-order rate equation and are plotted against [DnaK]. An independently determined value for $k_4^{obs}$ (the rate constant for release of ADP) in the presence of 5 mM $P_i$ is shown for comparison (●), since the *y*-intercept of the plot should be a measure of $k'_4$. The second-order rate constant for ADP association to DnaK was determined from a least-squares linear regression to be $1.6 \times 10^7$ M$^{-1}$ min$^{-1}$.

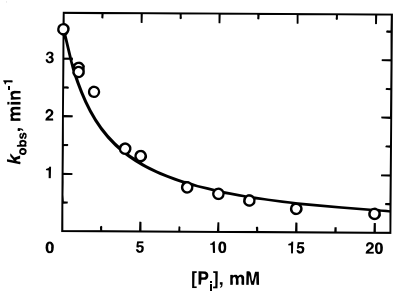


FIGURE 7: Measurement of the affinity of $P_i$ for DnaK as assessed by $P_i$-mediated inhibition of ATP binding. Reaction mixtures (100 $\mu$L) contained 3 nM ATP* (0.9 $\mu$Ci), 0.4 $\mu$M DnaK, and potassium phosphate as indicated. $K'_3$, the equilibrium dissociation constant for the binding of $P_i$ to free DnaK (not complexed with ADP), was determined from a fit of the data to eq 11 and was equal to 2.5 ± 0.3 mM.

of DnaK concentration (Figure 6) permitted an estimation of $k'_{-4}$ and $k'_4$ using eq 4, replacing $k_1$ and $k_{-1}$ by $k'_{-4}$ and $k'_4$, respectively, and omitting $k_2$. From this analysis, $k'_{-4} = (1.6 \pm 0.3) \times 10^7$ M$^{-1}$ min$^{-1}$, and $k'_4 < \sim 0.1$ min$^{-1}$; the value for $k'_4$ is consistent with the value ($\sim$0.03 min$^{-1}$) obtained from direct measurement at 5 mM $P_i$ (shown as a closed circle in Figure 6). A similar set of experiments performed in the presence of 1 mM $P_i$ yielded a similar second-order rate constant for binding, but a larger dissociation rate constant, $k_4^{obs}$ (data not shown), in agreement with the determined dependence of $k_4^{obs}$ on [$P_i$]. These results exclude the possibility of a large effect of $P_i$ on the rate of ADP binding. $K'_4$, the equilibrium dissociation constant of DnaK for ADP in the presence of phosphate, may be calculated from $k'_4/k'_{-4}$ and is approximately 1 nM, similar to the $K_D$ value obtained for ATP.

*Measurement of the Affinity of $P_i$ for DnaK.* Since $P_i$ does not affect the rate of ADP binding significantly, then the approximately 20-fold decrease in the release rate of ADP observed when significant levels of $P_i$ are present indicates that $P_i$ elicits a 20-fold increase in the affinity of DnaK for ADP. Completion of the thermodynamic cycle in Scheme 1 requires that ADP exert a similar effect on the affinity of $P_i$. Since $K_3K_4 = K'_3K'_4$, this relationship predicts that $K'_3$, the equilibrium dissociation constant of $P_i$ for free DnaK, should be $\sim$4 mM. To confirm this, we obtained a measure of $K'_3$ by taking advantage of our observation that the rate of ATP binding to DnaK is slowed by the presence of $P_i$. We preincubated a constant concentration of DnaK with a variable concentration of $P_i$, and measured the observed rate of ATP binding (Figure 7). The concentration of DnaK in the experiment (0.4 $\mu$M) is in the linear range for ATP binding (see Figure 3B), so a decrease in $k_{obs}$ monitors the fraction of DnaK unavailable for ATP binding. The data were adequately fit by eq 11, which describes competitive inhibition.

$$k_{obs} = \frac{k_1[\text{DnaK}]}{1 + \dfrac{[P_i]}{K_I}} \tag{11}$$

This analysis yielded a $K_I$ of 2.5 ± 0.3 mM, which is a measure of $K'_3$. This is similar to the expected value of $\sim$4 mM. We conclude that the binding of ADP and $P_i$ are thermodynamically coupled, since the presence of one increases the affinity of DnaK 10−20-fold for the other.

## DISCUSSION

We have performed steady-state and pre-steady-state kinetics experiments to quantitatively describe the ATPase cycle of DnaK. The results are adequately described by Scheme 1, and the kinetic parameters obtained are summarized in Table 1. We have found that DnaK binds ATP tightly, with a $K_D$ of approximately 1 nM. Hydrolysis of ATP, or a first-order step preceding hydrolysis, is rate limiting in the steady state under typical *in vitro* conditions. However, if physiological concentrations of $P_i$ are present, release of ADP product becomes partially rate limiting for the DnaK ATPase cycle.

*Hydrolysis Is Rate Limiting in the Absence of Exogenous $P_i$.* Recently, an alternative kinetic model for the ATPase cycle of DnaK has been published (*39*, *40*), which differs in that hydrolysis of ATP is postulated to be a rapid step, leading to the formation of a "DnaK*ADP" state, which is detectable by a change in the intrinsic fluorescence of DnaK. Dissociation of ADP from this complex is postulated to be slow and rate limiting for the overall cycle. Our data exclude a model in which ATP hydrolysis is fast relative to the overall cycle. The rate constant for hydrolysis, $k_2$, is approximately equal to $k_{cat}$, inconsistent with a model in which a step after hydrolysis is rate determining. Furthermore, in the absence of exogenous $P_i$, the vast majority of DnaK isolated in steady state was complexed with ATP rather than ADP. This finding is also inconsistent with a model in which ADP release is rate limiting, which predicts that ADP should accumulate at the active site. The differences between the models cannot be attributed to differences in $P_i$ concentration, since (1) the experiments that led to the model with ADP release being rate limiting were conducted in the absence of added $P_i$ (*39*, *40*), and (2) even in the presence of significant concentrations of $P_i$ (e.g., 5 mM, 20-fold over $K_3$), ADP release is not slower than ATP hydrolysis ($k'_4 \approx k_2$) and so is not fully rate limiting. We suggest that the fluorescence change attributed to formation of the "DnaK*ADP" state following rapid ATP hydrolysis may represent a conforma-

tional change induced by the binding of ATP, analogous to that observed for bovine Hsc70 (*41*). A recent report by Pierpaoli *et al*. (*42*) reached the same conclusion, based in part on evidence that the DnaK preparations used in the earlier studies (*39*, *40*) may have contained significant amounts of bound ADP, which would cause a substantial slowing in the rate of ATP binding and complicate assignment of changes in the fluorescence of DnaK.

*A Kinetic Balance between ATP Hydrolysis and ADP Release.* By establishing a kinetic framework for the ATPase cycle, we expected to gain insight into the functioning of DnaK *in vivo*. To this end, it is important to understand the kinetics under physiologically relevant conditions, which will permit estimation of the relative concentrations of ATP-bound and ADP-bound forms of DnaK. DnaK·ATP is "activated" in the sense that it rapidly binds and releases peptide substrates (*17*), whereas DnaK·ADP may exist largely in stable complexes containing peptide substrates. Although ATP hydrolysis is fully rate limiting under typical *in vitro* conditions, in the presence of physiological concentrations of $P_i$ [5−10 mM (*43*, *44*)], the rate of ADP release is greatly diminished, to a level where the rate of ADP dissociation contributes significantly to the overall rate of the intrinsic DnaK ATPase cycle. In the absence of other influences *in vivo*, a significant fraction of DnaK at steady state would be predicted to exist in the ADP-bound form. Though peptide substrates and the DnaJ and GrpE cochaperone proteins also affect the kinetics of the ATPase cycle and are likely to exert significant effects on the ratio of the two forms of DnaK, the results presented here provide a relevant baseline for evaluating these additional effects.

*In vivo*, in the presence of a significant $P_i$ concentration, the kinetics of the ATPase cycle may qualitatively resemble the kinetics of the GTP binding and hydrolysis cycle of the Ras superfamily of low molecular weight GTP-binding proteins. These proteins function as molecular switches in such processes as regulation of cell growth and differentiation, and cytoskeletal organization. They function while in their GTP-bound state by acting on downstream effectors and then return to an inactive state upon hydrolysis of GTP (for reviews, see refs *45* and *46*). Like DnaK, these proteins bind nucleotide tightly, and hydrolyze it slowly. One of the best characterized members, Ras, hydrolyzes GTP with a rate constant of ∼0.02 $min^{-1}$ at 37 °C (*47*), several fold slower than DnaK at this temperature (Figure 2B). Though the rate constants for hydrolysis and product release vary among GTP-binding proteins, for many individual family members, including Ras, the rate constants for GTP hydrolysis and GDP release are comparable to each other (*47*, *48*). This balance appears to be important for the functioning of Ras, since mutations that alter the balance, either by decreasing the intrinsic GTP hydrolysis rate or increasing the GDP/GTP exchange rate, are oncogenic (*49*, *50*). Additionally, the nucleotide binding/hydrolysis cycles of Ras and DnaK are similar in another respect. GTP-binding proteins function *in vivo* in cooperation with distinct regulators of the nucleotide binding and hydrolysis cycle, including proteins responsible for stimulating specifically nucleotide hydrolysis (*51*, *52*) or product release (*48*). The DnaJ and GrpE cochaperones fulfill these respective roles for the DnaK ATPase. If it is presumed that the intrinsic equilibrium between the ATP-bound and ADP-bound forms of DnaK is approximately 1 *in vivo*, then DnaJ action would drive the equilibrium to the ADP-bound form by stimulating nucleotide hydrolysis (*25*, *26*, *42*), whereas GrpE would drive it to the ATP-bound form by stimulating product release (*25*, *27*).

*Two-Step ATP Binding.* It has been suggested that a conformational change of DnaK occurs, following initial ATP binding, based on an altered protease digestion pattern in the presence of ATP (*53*−*55*) and short angle X-ray scattering data (*56*). Additionally, it has been shown that ATP binding to Hsc70 proceeds in two steps based on stopped-flow fluorescence data (*41*); this was interpreted as a conformational change following the formation of an initial collision complex, with the equilibrium for the first-order step lying far to the right (i.e., essentially all DnaK·ATP complexes exist in the postconformational-change state). Experiments presented here examining the association of ATP with DnaK showed that with excess DnaK, at concentrations ranging from 20 nM to 1 $\mu$M, the reaction followed pseudo-first-order kinetics, consistent with a one-step binding mechanism, as indicated in Scheme 1. This analysis, however, does not rule out a multiple-step binding mechanism. If DnaK also binds ATP in two steps, the values that we have obtained for $k_1$ and $k_{-1}$ would correspond, not to true microscopic rate constants, but rather to combinations of rate constants representing both steps. Nevertheless, $k_{-1}/k_1$ would still provide an accurate estimation of $K_D$, which would also be described by a combination of rate constants representing both steps.[4]

*A Conformational Change Associated with ATP Hydrolysis*? By performing single-turnover experiments at various temperatures, we were able to obtain an estimate of the activation energy for the hydrolysis step ($k_2$) specifically. The measured value of ∼26 kcal/mol is larger than has been observed for several enzymes with nucleoside triphosphate hydrolase activity [including the GTP-binding protein Ras, which hydrolyzes GTP even more slowly than DnaK hydrolyzes ATP (*57*)], and is roughly equal to the activation energy for the nonenzymatic hydrolysis of ATP (*58*, *59*). It is possible that, rather than reflecting the chemical step per se, this activation energy instead primarily reflects a conformational change associated with hydrolysis of ATP (distinct from the conformational change associated with the binding of ATP). This putative conformational change associated with ATP hydrolysis may well be responsible for the observed higher affinity of peptides for the ADP-bound form of DnaK, and could represent essentially the reverse of the change that occurs upon ATP binding. The conformational change could be rate limiting for hydrolysis, in which case $E_a$ measures the temperature dependence of this step directly. Alternatively, an unfavorable conformational change may precede rate limiting chemistry, in which case $k_2 \approx K_{conf}\, k_{chem}$ and $E_a$ includes the temperature dependence of the conformational-change equilibrium. Consistent with the notion that a conformational change of DnaK associated with ATP hydrolysis could have a large kinetic activation

[4] Assuming the equilibrium for a conformational change subsequent to initial complex formation lies far to the right as observed for Hsc70 ($k_1^* \gg k_{-1}^*$ where $k_1^*$ and $k_{-1}^*$ refer to the forward and reverse rate constants for the conformational change, respectively), the determined rate constant for ATP release is $\sim k_{-1}^* k_{-1}/(k_{-1} + k_1^*)$. The determined rate constant for binding is $\sim k_1 k_1^*/(k_{-1} + k_1^*)$, so $k_{off}/k_{on} \approx k_{-1}k_{-1}^*/k_1 k_1^*$, approximately equal to $K_D$.

barrier, activation energies for various other conformational changes of Hsp70 proteins have been measured and were also found to be large. For example, the second step of ATP binding to Hsc70 has been interpreted to be a conformational change with an activation energy of 40 ± 1 kcal/mol (*41*). Moreover, binding and release of peptides by Hsp70 are thought to involve conformational changes (*19*). A peptide (MQERITLKDYAM) derived from the λ Cro protein was shown to bind DnaK with an activation energy of 26 ± 8 kcal/mol, and its release was found to have an activation energy of 34.6 ± 1.2 kcal/mol (*60*). It may be these types of structural rearrangements that are rate limiting for Hsp70 action, as reflected in the large activation energies. A conformational change associated with ATP hydrolysis would be consistent with the observed stimulation of ATP hydrolysis by peptides, which are known to interact with the C-terminal domain of DnaK, a locale spatially distinct from the site of nucleotide hydrolysis on the N-terminal domain. An effect of peptides on a conformational change would seem to be more feasible physically than a direct effect on catalysis. We infer that peptide binding either accelerates a rate limiting conformational step that precedes chemistry or alters the equilibrium of an unfavorable conformational step that precedes rate limiting chemistry.

*Comparison of DnaK with Eukaryotic Hsc70 and Mitochondrial Hsp70.* Comparison of our results with those from a study of the ATPase kinetics of Hsc70 (*35*, *41*) reveals differences between the two proteins. For both DnaK and Hsc70, hydrolysis of ATP has been found to proceed slowly and to contribute to the overall rate. However, $P_i$ release from Hsc70 was determined to be slow as well, and to be partially rate limiting, even in the absence of exogenous $P_i$. Furthermore, the Hsc70 ADP release rate was found to be several fold faster than that measured here for DnaK (1.7 $min^{-1}$ vs 0.4 $min^{-1}$ for DnaK). A more significant difference between these proteins is their affinity for ATP, where the $K_D$ for Hsc70 was calculated to be 42 nM, 40-fold weaker than the 1 nM $K_D$ we have calculated for DnaK. This disparity primarily results from a large difference in the ATP release rate, which for Hsc70 is ∼0.7 $min^{-1}$, nearly 100-fold faster than release of ATP from DnaK. For Hsc70, ATP release is several fold faster than hydrolysis, so the ATP-binding step is essentially in rapid equilibrium. In contrast, release of ATP from DnaK is slower than hydrolysis, so this system is more closely approximated by the limiting case of irreversible binding. It is interesting in this regard that GrpE interacts with DnaK and increases the rate of ATP release[5] as well as ADP release (*25*). In effect, GrpE action converts the DnaK ATP-binding step to a rapid equilibrium, qualitatively more similar to the intrinsic ATPase cycle of Hsc70. Although a homologue of GrpE has been found in the matrix of yeast mitochondria, there are apparently no GrpE homologues in the cytosol of eukaryotic cells (at least in *S. cerevisiae*, whose genome has been entirely sequenced). Variations in the kinetic properties of the intrinsic ATPase cycles between prokaryotic and eukaryotic Hsp70 proteins may thus underlie the requirement in prokaryotes for GrpE, which appears to function largely or entirely by affecting the kinetics of the cycle. Perhaps because of the intrinsically faster rate of nucleotide exchange for Hsc70, there may be no physiological need in the cytosol of eukaryotic cells for a GrpE-like cochaperone.

Mitochondrial matrix Hsp70 protein, on the other hand, is assisted in its action as a molecular chaperone by Mge1 protein, a mitochondrial GrpE homologue. Because of its dependence on a GrpE-like cochaperone, mitochondrial Hsp70 is apparently more similar to DnaK functionally than eukaryotic Hsc70. A recent report, published after this work was completed, concludes that the presence of inorganic phosphate inhibits the intrinsic ATPase activity of mitochondrial Hsp70 by slowing the release of ADP (*61*). Although this response to inorganic phosphate is similar to that reported here for DnaK, there apparently remain significant differences between the behavior of DnaK and mitochondrial Hsp70. For example, the intrinsic ATPase turnover number of mitochondrial Hsp70 was reported to be more than 10-fold higher than that of DnaK, and product release from this Hsp70 was judged to be strictly ordered, with $P_i$ always dissociating prior to ADP (*61*).

*Comparison with Other Kinetic Studies of the DnaK ATPase.* After this work was completed, an investigation of the intrinsic and peptide-stimulated ATPase activity of DnaK was reported (*20*). Theyssen *et al*. performed both steady-state analysis of the DnaK ATPase and transient stopped-flow analysis of the interaction of DnaK with fluorescent nucleotide analogs of ADP and ATP. Consistent with the results reported here, Theyssen *et al*. found that ATP hydrolysis is rate limiting for the intrinsic ATPase cycle and that ATP is released more slowly than it is hydrolyzed. Earlier, McCarty *et al*. (*62*) had demonstrated that ATP is the primary nucleotide bound to DnaK during a steady-state reaction and, based on this finding, they also concluded that the ATP hydrolysis step is rate limiting.

There are, however, differences between our findings and those of Theyssen *et al*. (*20*) that merit further discussion. Theyssen *et al*. observed only a minor effect of $P_i$ on the release rate of ADP (about a 2-fold slowing of the rate at 2 mM $P_i$). In contrast, we observed nearly a 20-fold decrease in the ADP-release rate at this concentration of $P_i$. The underlying basis for this difference is not clear; nevertheless, we confirmed that our conclusion is correct by demonstrating that $P_i$ affects the ATP/ADP ratio of the nucleotide bound to DnaK during steady-state hydrolysis of ATP. If $P_i$ at 2 mM exerted only a 2-fold slowing of the ADP release rate (e.g., to 0.18 $min^{-1}$), ATP hydrolysis, with a $k_2$ of 0.018 $min^{-1}$, would remain almost fully rate limiting and bound ADP should not accumulate. In sharp contrast to this expectation, however, nearly half of the bound nucleotide was ADP at 2 mM $P_i$ (Table 2). This shows that ADP release is partially rate limiting under these conditions (i.e., the release rate for ADP must be slowed approximately 20-fold, since $P_i$ had no significant effect on the hydrolysis rate of ATP). We also note that the increase in affinity of DnaK for ADP when exogenous $P_i$ is present correlates well with the ∼12-fold effect of ADP on the affinity of DnaK for $P_i$. Thus, all of our observations are consistent with a model in which the binding of ADP and $P_i$ are thermodynamically coupled, with a coupling energy of ∼1.6 kcal/mol (equivalent to a 10−20-fold increase in affinity when both ADP and exogenous $P_i$ are present). Theyssen *et al*. also reported observing a tight-binding mode of $P_i$ ($K_D$ = 0.45 μM) by monitoring changes in Trp fluorescence which resulted from

[5] R. Russell and R. McMacken, unpublished data.

a slow conformational change of the DnaK·ADP·$P_i$ complex ($k_{obs} = 0.05$ min$^{-1}$). We did not observe this state, perhaps because it is only visible spectroscopically. Regardless, since this form is postulated to be bypassed in the steady-state (*20*), its physiological significance is uncertain.

A comparison of the rate constants reported here with those determined, chiefly with complementary methods, by Theyssen *et al*. (*20*) reveals similarities in certain relative rate constants. For example, Theyssen *et al*. set an upper limit of 7.3 nM for the $K_D$ of ATP, as calculated from the kinetic rate constants for ATP binding and release. This value is consistent with the $K_D$ value of 1.0 ± 0.3 nM we found using a comparable analysis. It is notable, however, that the magnitudes of several of the DnaK rate constants reported here are approximately 5−6-fold lower than those determined by Theyssen *et al*. (measured at similar temperature and pH). For example, Theyssen *et al*. reported rate constants of 0.1 min$^{-1}$ for ATP hydrolysis, <0.1 min$^{-1}$ for ATP release, and 2 min$^{-1}$ for ADP release (*20*). It is unlikely that the substantially lower rates reported here are due to the presence of significant levels of inactive protein in our DnaK preparations. Our rate constants were determined under pre-steady-state conditions with saturating DnaK and these values would be expected to be relatively insensitive to the presence of some inactive protein. Additionally, steady-state ATP hydrolysis rates of 0.02 min$^{-1}$, nearly identical to the rate found here, have been reported previously by other laboratories (*34*, *63*). One possible explanation for the rate discrepancies might be the presence of small amounts of contaminating peptide or polypeptide in the DnaK prepartion used by Theyssen *et al*. In our experience, minor contamination of DnaK with peptides is difficult to avoid. In fact, peptides are not resolved effectively from DnaK in our preparations until the final chromatographic step[6] (chromatography on a Mono-Q resin). It is known that peptides stimulate ATP hydrolysis by Hsp70 proteins (*21*, *22*). Additionally, the presence of peptides has been found to stimulate the rate of release of ATP from DnaK 10-fold[5] as well as enhance the rate of release of ADP from bovine Hsc70 (*19*). This explanation for the differences in the magnitudes of the rate constants assigned to the basic DnaK ATPase cycle is also consistent with the fact that both we[5] and Theyssen *et al*. find a similar rate constant for ATP hydrolysis (~0.6 min$^{-1}$) when our individual DnaK preparations are maximally stimulated with saturating concentrations of peptide.

## ACKNOWLEDGMENT

We thank Wali Karzai and Andrew Mehl for numerous helpful discussions. We also are grateful to Cecile Pickart and Dan Herschlag for critical reviews of the manuscript.

## SUPPORTING INFORMATION AVAILABLE

Construction of plasmid pRLM163, protocol for overexpression of DnaK, protocol for purification of DnaK (7 pages). Ordering information is given on any current masthead page.

## REFERENCES

1. McKay, D. B. (1993) *Adv. Protein Chem. 44*, 67−98.
2. Georgopoulos, C., and Welch, W. J. (1993) *Annu. Rev. Cell Biol. 9*, 601−634.
3. Hartl, F. U. (1996) *Nature 381*, 571−579.
4. Rothman, J. E. (1989) *Cell 59*, 591−601.
5. Hendrick, J. P., and Hartl, F. U. (1993) *Annu. Rev. Biochem. 62*, 349−384.
6. Deshaies, R. J., Koch, B. D., Werner-Washburne, M., Craig, E. A., and Schekman, R. (1988) *Nature 332*, 800−805.
7. Chirico, W. J., Waters, M. G., and Blobel, G. (1988) *Nature 332*, 805−810.
8. Straus, D., Walter, W., and Gross, C. A. (1990) *Genes Dev. 4*, 2202−2209.
9. Liberek, K., Georgopoulos, C., and Zylicz, M. (1988) *Proc. Natl. Acad. Sci. U.S.A. 85*, 6632−6636.
10. Alfano, C., and McMacken, R. (1989) *J. Biol. Chem. 264*, 10709−10718.
11. Chappell, T. G., Konforti, B. B., Schmid, S. L., and Rothman, J. E. (1987) *J. Biol. Chem. 262*, 746−751.
12. Landry, S. J., Jordan, R., McMacken, R., and Gierasch, L. M. (1992) *Nature 355*, 455−457.
13. Zhu, X., Zhao, X., Burkholder, W. F., Gragerov, A., Ogata, C. M., Gottesman, M. E., and Hendrickson, W. A. (1996) *Science 272*, 1606−1614.
14. Flaherty, K. M., DeLuca-Flaherty, C., and McKay, D. B. (1990) *Nature 346*, 623−628.
15. Harrison, C. J., Hayer-Hartl, M., Di Liberto, M., Hartl, F., and Kuriyan, J. (1997) *Science 276*, 431−435.
16. Palleros, D. R., Reid, K. L., Shi, L., Welch, W. J., and Fink, A. L. (1993) *Nature 365*, 664−666.
17. Schmid, D., Baici, A., Gehring, H., and Christen, P. (1994) *Science 263*, 971−973.
18. Greene, L. E., Zinner, R., Naficy, S., and Eisenberg, E. (1995) *J. Biol. Chem. 270*, 2967−2973.
19. Takeda, S., and McKay, D. B. (1996) *Biochemistry 35*, 4636−4644.
20. Theyssen, H., Schuster, H. P., Packschies, L., Bukau, B., and Reinstein, J. (1996) *J. Mol. Biol. 263*, 657−670.
21. Flynn, G. C., Chappell, T. G., and Rothman, J. E. (1989) *Science 245*, 385−390.
22. Jordan, R., and McMacken, R. (1995) *J. Biol. Chem. 270*, 4563−4569.
23. Baker, T. A., and Wickner, S. H. (1992) *Annu. Rev. Genet. 26*, 447−477.
24. Schroder, H., Langer, T., Hartl, F. U., and Bukau, B. (1993) *EMBO J. 12*, 4137−4144.
25. Liberek, K., Marszalek, J., Ang, D., Georgopoulos, C., and Zylicz, M. (1991) *Proc. Natl. Acad. Sci. U.S.A. 88*, 2874−2878.
26. Karzai, A. W., and McMacken, R. (1996) *J. Biol. Chem. 271*, 11236−11246.
27. Packschies, L., Theyssen, H., Buchberger, A., Bukau, B., Goody, R. S., and Reinstein, J. (1997) *Biochemistry 36*, 3417−3422.
28. Cyr, D. M., Lu, X., and Douglas, M. G. (1992) *J. Biol. Chem. 267*, 20927−20931.
29. Prasad, K., Barouch, W., Greene, L., and Eisenberg, E. (1993) *J. Biol. Chem. 268*, 23758−23761.
30. Ungewickell, E., Ungewickell, H., Holstein, S. E., Lindner, R., Prasad, K., Barouch, W., Martin, B., Greene, L. E., and Eisenberg, E. (1995) *Nature 378*, 632−635.
31. Bolliger, L., Deloche, O., Glick, B. S., Georgopoulos, C., Jeno, P., Kronidou, N., Horst, M., Morishima, N., and Schatz, G. (1994) *EMBO J. 13*, 1998−2006.
32. Laloraya, S., Gambill, B. D., and Craig, E. A. (1994) *Proc. Natl. Acad. Sci. U.S.A. 91*, 6481−6485.

[6] W. Karzai, R. Russell, and R. McMacken, unpublished data.

33. Gao, B., Greene, L., and Eisenberg, E. (1994) *Biochemistry 33*, 2048−2054.
34. Burkholder, W. F., Panagiotidis, C. A., Silverstein, S. J., Cegielska, A., Gottesman, M. E., and Gaitanaris, G. A. (1994) *J. Mol. Biol. 242*, 364−377.
35. Ha, J. H., and McKay, D. B. (1994) *Biochemistry 33*, 14625−14635.
36. McCarty, J. S., and Walker, G. C. (1991) *Proc. Natl. Acad. Sci. U.S.A. 88*, 9513−9517.
37. Montgomery, D., Jordan, R., McMacken, R., and Freire, E. (1993) *J. Mol. Biol. 232*, 680−692.
38. Gao, B., Emoto, Y., Greene, L., and Eisenberg, E. (1993) *J. Biol. Chem. 268*, 8507−8513.
39. Banecki, B., Liberek, K., Wall, D., Georgopoulos, C., Bertoli, E., Tanfani, F., and Zylicz, M. (1996) *J. Biol. Chem. 271*, 14840−14848.
40. Banecki, B., and Zylicz, M. (1996) *J. Biol. Chem. 271*, 6137−6143.
41. Ha, J. H., and McKay, D. B. (1995) *Biochemistry 34*, 11635−11644.
42. Pierpaoli, E. V., Sandmeier, E., Baici, A., Schonfeld, H. J., Gisler, S., and Christen, P. (1997) *J. Mol. Biol. 269*, 757−768.
43. Kashket, E. R. (1982) *Biochemistry 21*, 5534−5538.
44. Rao, R. N., Roberts, M. F., Torriani, A., and Yashphe, J. (1993) *J. Bacteriol. 175*, 74−79.
45. Bourne, H. R., Sanders, D. A., and McCormick, F. (1990) *Nature 348*, 125−132.
46. Bourne, H. R., Sanders, D. A., and McCormick, F. (1991) *Nature 349*, 117−127.
47. Neal, S. E., Eccleston, J. F., and Webb, M. R. (1990) *Proc. Natl. Acad. Sci. U.S.A. 87*, 3562−3565.
48. Leonard, D. A., Evans, T., Hart, M., Cerione, R. A., and Manor, D. (1994) *Biochemistry 33*, 12323−12328.
49. Reinstein, J., Schlichting, I., Frech, M., Goody, R. S., and Wittinghofer, A. (1991) *J. Biol. Chem. 266*, 17700−17706.
50. Colby, W. W., Hayflick, J. S., Clark, S. G., and Levinson, A. D. (1986) *Mol. Cell Biol. 6*, 730−734.
51. Moore, K. J. M., Webb, M. R., and Eccleston, J. F. (1993) *Biochemistry 32*, 7451−7459.
52. Nomanbhoy, T. K., Leonard, D. A., Manor, D., and Cerione, R. A. (1996) *Biochemistry 35*, 4602−4608.
53. Buchberger, A., Theyssen, H., Schroder, H., McCarty, J. S., Virgallita, G., Milkereit, P., Reinstein, J., and Bukau, B. (1995) *J. Biol. Chem. 270*, 16903−16910.
54. Kamath-Loeb, A. S., Lu, C. Z., Suh, W. C., Lonetto, M. A., and Gross, C. A. (1995) *J. Biol. Chem. 270*, 30051−30059.
55. Banecki, B., Zylicz, M., Bertoli, E., and Tanfani, F. (1992) *J. Biol. Chem. 267*, 25051−25058.
56. Shi, L., Kataoka, M., and Fink, A. L. (1996) *Biochemistry 35*, 3297−3308.
57. Schweins, T., Geyer, M., Kalbitzer, H. R., Wittinghofer, A., and Warshel, A. (1996) *Biochemistry 35*, 14225−14231.
58. Admiraal, S. J., and Herschlag, D. (1995) *Chem. Biol. 2*, 729−739.
59. Couture, A. M., and Ouellet, L. (1957) *Can. J. Chem. 35*, 1248−1253.
60. Farr, C. D., Galiano, F. J., and Witt, S. N. (1995) *Biochemistry 34*, 15574−15582.
61. Dekker, P. J. T., and Pfanner, N. (1997) *J. Mol. Biol. 270*, 321−327.
62. McCarty, J. S., Buchberger, A., Reinstein, J., and Bukau, B. (1995) *J. Mol. Biol. 249*, 126−137.
63. Buchberger, A., Valencia, A., McMacken, R., Sander, C., and Bukau, B. (1994) *EMBO J. 13*, 1687−1695.

BI972025P